Detailed Diagnostics of the BIOMASS Feed Array Prototype

Cappellin, C.; Pivnenko, Sergey; Pontoppidan, K.

Published in:
Proceedings of the 35th Annual Symposium of the Antenna Measurement Techniques Association

Publication date:
2013

Document Version
Publisher's PDF, also known as Version of record

Detailed Diagnostics of the BIOMASS Feed Array Prototype

C. Cappellin[1], S. Pivnenko[2], K. Pontoppidan[1]
[1]TICRA, Læderstræde 34, DK-1201 Copenhagen, Denmark
[2]DTU Elektro, Technical University of Denmark, Ørsteds Plads, Building 348, 2800 Kgs. Lyngby, Denmark

Abstract—**The 3D reconstruction algorithm of DIATOOL is applied to the prototype feed array of the BIOMASS synthetic aperture radar, recently measured at the DTU-ESA Spherical Near-Field Antenna Test Facility in Denmark. Careful analysis of the measured feed array data had shown that the test support frame of the array had a significant influence on the measured feed pattern. The 3D reconstruction and further post-processing is therefore applied both to the feed array measured data, and a set of simulated data generated by the GRASP software which replicate the series of measurements. The results of the diagnostics and the corresponding improvement of the feed array field obtained by removal of the undesired effect of the frame are presented and discussed.**

I. INTRODUCTION

Accurate and general antenna diagnostics techniques have in recent years attracted the interest of the antenna measurements community. Several algorithms and two commercial software tools have been developed with the purpose of identifying from the radiated measured field the electrical and mechanical errors affecting the performances of the antenna under test. DIATOOL from TICRA is one of the available commercial software tools. One of its key features is its 3D reconstruction algorithm, which, with its higher-order Method of Moments-based implementation, makes it possible to reconstruct field and surface currents on arbitrary 3D surfaces enclosing the AUT [1]-[2].

An important feature of the 3D reconstruction algorithm of DIATOOL is the ability of identifying the undesired sources of radiation and scattering, such as for example leaking cables and antenna support structures, which can affect the performances of the antenna. Of particular interest is the subsequent filtering of this undesired radiation, to obtain a more accurate measured field.

The purpose of the work described in this paper is to apply the 3D reconstruction algorithm of DIATOOL with filtering of the undesired radiation to the prototype feed array of the BIOMASS synthetic aperture radar. The prototype feed array was recently measured at the DTU-ESA Spherical Near-Field Antenna Test Facility in Denmark and showed a too strong and unacceptable effect of the structure used to mount the antenna on the antenna positioner.

The BIOMASS candidate mission underwent in the past years an extensive feasibility study and was selected in May 2013 to become the seventh Earth Explorer programme of the European Space Agency [3]. The main payload of the BIOMASS is a P-band (435 MHz) synthetic aperture radar constituted by a very large deployable reflector of projected aperture of approximately 11 m X 10 m [4]. The reflector antenna is illuminated by a small feed array, in the following called prototype feed array, as illustrated in Figure 1. It is a dual-polarized feed, consisting of a 2×2 patch array of about 1 m^2 located on a satellite, whose dimensions are about 1×1.5×3 m^3.

The paper is organized as follows: in Section 2 the measured field of the prototype feed array is shown and discussed. In Section 3 a GRASP model of the feed array is made and simulated fields that replicate the measured fields are produced. In Section 4 the 3D reconstruction of DIATOOL is applied to these synthetic data and in Section 5 to the measured data. In both cases, the effect of the structure used to mount the antenna on the antenna positioner will be filtered out. Conclusions will finally be drawn in Section 6.

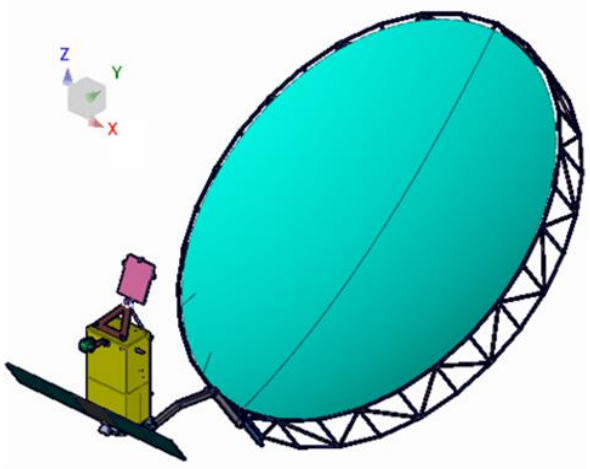

Figure 1. The feed array (in pink), the satellite body (in yellow) and the large deployable reflector (in cyan).

II. THE PROTOTYPE FEED ARRAY

The prototype feed array of the BIOMASS consists of four square patches, properly excited, and located on a rectangular ground plane, see Figure 2. The feed array was recently measured at the DTU-ESA Spherical Near-Field Antenna Test Facility [5], with the aim at establishing an optimum on-ground performance verification methodology for the BIOMASS payload [6]. After considering different approaches, a two-step methodology was proposed, which consisted of a measurement of the radiation pattern and radiation efficiency of the prototype feed array alone, and a subsequent calculation of the radiation pattern and gain of the entire antenna using the GRASP software.

To mount the feed array antenna on the antenna positioner, an appropriate and stiff test support structure was designed and manufactured, as shown in Figure 2. The test support structure is a rectangular frame of square aluminium tubes with outer dimensions of 50 mm X 50 mm. Its effect on the measured radiation characteristics was unknown.

To study the effect of the test support frame, two measurement set-ups were therefore considered, see Figure 3. In configuration A the test support frame was located 100 mm behind the feed array, while in configuration B the distance was set to 400 mm.

Figure 2. The feed array and its test support frame.

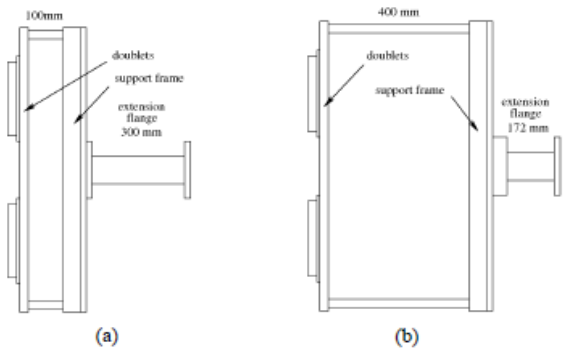

Figure 3. Measurement configuration A (left side), and measurement configuration B (right side).

The amplitude of the measured field for phi=0 deg is shown in Figure 4. It is seen that noticeable differences appear for theta between 90 deg and 180 deg. At the same time, a slight shift of the first sidelobe is observed. Similar behaviors were noted in other phi cuts. These differences are not surprising and are mainly due to the different scattering of the test support frame in the backward hemisphere. The main concern is the effect of the test support frame in the main beam, i.e. in the angular region $\theta \in [0, 35]$ deg, corresponding to the illumination of the reflector. In order to quantify the difference between the patterns by a single number, the complex difference between the measured fields from configuration A and B was calculated and plotted as a black curve in Figure 4. The complex difference has a maximum at -14 dBi, thus about 29 dB below the pattern peak of 14.8 dBi, in the angular region $\theta \in [0, 35]$ deg. This gives rise to a peak-to-peak variation of the measured pattern of ±0.3 dB at the pattern peak level, which is a too large value in itself, and also relative to the other uncertainty contributions of the applied measurement technique.

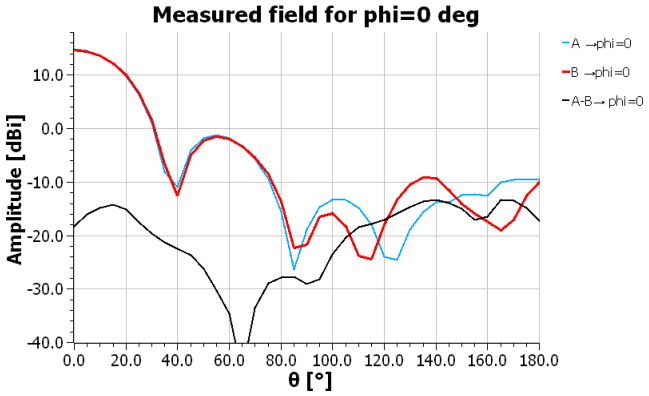

Figure 4. Amplitude of the measured field for phi=0 deg, and configuration A (in blue) and B (in red).

We know that both measurements are not precise, since they include the effect of the test support frame, which will not be present in the final satellite configuration. In view of the difference seen in Figure 4, few questions were thus posed. What is the contribution of the test support structure to the "true" radiated field of the feed array? Is configuration A more accurate than B, or vice versa? Is it possible to obtain a better result by removing or reducing the effect of the test support frame through an appropriate post-processing?

The purpose of the present paper and the following sections is therefore manifold: first, estimate the effect of the used test support frame, through simulations; second, use DIATOOL to investigate if the effect of the test support frame can be removed from the measured patterns of Figure 4. Third, prove that the cleaned pattern provided by DIATOOL is better than the measured field, i.e. it is closer to the "true" pattern of the prototype feed array. If these three conclusions can be drawn, the cleaned pattern provided by DIATOOL can then be used to illuminate the large deployable reflector in GRASP, and thus provide the required overall performances of the P-band synthetic aperture radar.

III. GRASP MODEL OF THE PROTOTYPE FEED ARRAY

To begin with, a GRASP model of the prototype feed array was made. It consists of a tabulated mesh describing the four patches, the ground plane and the metallic support frame. Method of Moments (MoM) is used to compute the radiated field. An additive noise with SNR equal to 60 dB is also considered. This simulates the measurements performed at the DTU-ESA facility and accounts for the effect of the support frame. The field is computed twice, once for configuration A and once for configuration B. A sketch of the feed array geometry, with the radiating frame of configuration B is shown in Figure 5.

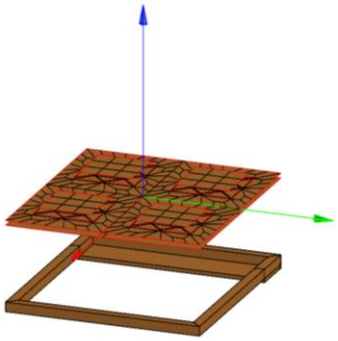

Figure 5. GRASP model of the feed array prototype with frame B.

A plot of the two patterns for phi=0 deg is shown in Figure 6, together with the complex difference of the two fields. By comparing Figure 6 with Figure 4 we see that the blue and red curves are similar, especially in the main beam and first sidelobe. However, the amplitude of the complex difference has now a peak value of -24 dBi in the main beam region, which gives rise to a peak-to-peak variation of ±0.1 dB at the pattern peak level. This means that in theory the field radiated by configuration A is very similar to the one radiated by configuration B. The complex difference of Figure 4 showed however a maximum of -14 dBi, i.e. 10 dB of difference. We can therefore conclude that the measured data include the effect of some non-idealities, which are not present in the GRASP model. Examples of such non-idealities can be an unwanted radiation of the array feeding network, or the honeycomb dielectric of the patch array (modeled as air in the GRASP model). An unwanted radiation of the array feeding network is considered of special importance, since it will illuminate the support frame and the patch array, increasing therefore the differences between configuration A and B.

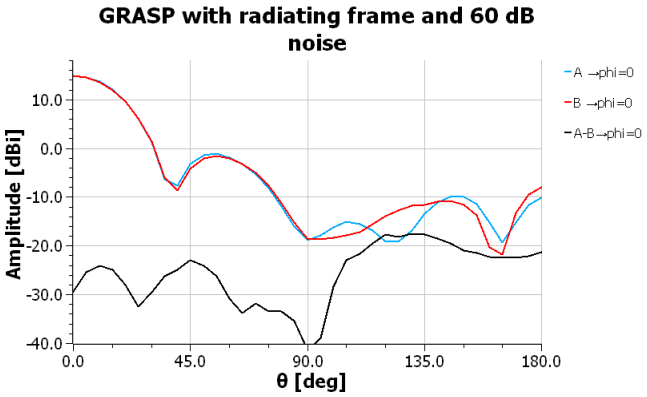

Figure 6. Amplitude of the field obtained by GRASP with MoM, with radiating feed array and support frame, and an additive noise of SNR=60 dB.

It was therefore decided to introduce in the GRASP model four *x*- and *y*-oriented magnetic dipoles, located just behind the patch array. The excitation of the dipoles was set with the purpose to obtain a difference pattern between configuration A and B with a peak around -14 dBi, as seen in Figure 4, without necessarily reproducing exactly the measured field. The new patterns are shown in Figure 7, where it is seen that now the amplitude of the complex difference has a peak of -11 dBi, which is now acceptable (Job 5).

Job	Field computation
Job 5	Field is given by the currents on the frame and patch array when illuminated by the generators and the dipoles, with coupling between frame and patch array included, plus dipoles
Job 10	Field is given by the currents on the patch array when illuminated by the generators and the dipoles, with coupling between frame and patch array included, plus dipoles
Job 22	Field is given by the currents on the patch array when illuminated by the generators and the dipoles, plus dipoles

Table 1. Summary of Job and corresponding field computations.

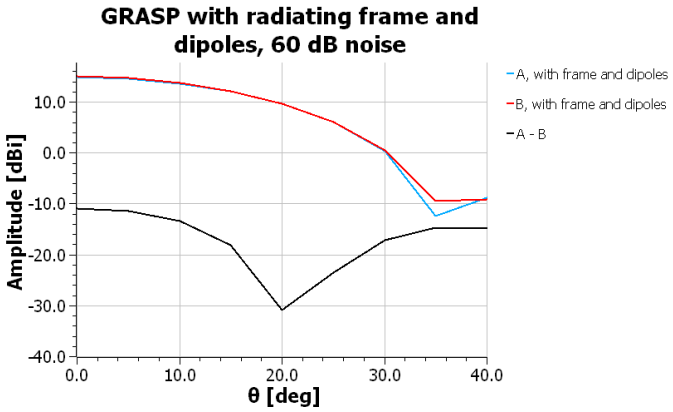

Figure 7. Amplitude of the field obtained by GRASP with MoM, with radiating feed array, support frame and eight magnetic dipoles and an additive noise of SNR=60 dB.

The above GRASP model was finally used to compute two more patterns. The first one is the field given by the dipoles and the patch array, and a non-radiating frame. It is noted that the coupling between the frame and the patch array was considered (Job 10). It was found that the difference between configuration A and B had a value of -10 dBi in the main beam region, i.e. the coupling between the patch array and the frame varies significantly from configuration A and B.

The second and last pattern is given by the patch array and the dipoles, without frame (Job 22), i.e. an ideal reference. A difference between Job 10 and Job 22, see Figure 8, is a measure of the coupling between the frame and the patch array, once the patch array is illuminated by the dipoles and the patch array excitation. It is seen that the coupling is clearly higher for configuration A than B. It means that for configuration A the currents on the patch array when the frame is present vary more relative to the case where the frame is not present. A difference between Job 5 and Job 22 is a measure of the field radiated by the frame once illuminated by the dipoles and the patch excitation, and of the coupling between

frame and patch array, see Figure 9. It seems that there is no difference between configuration A and B, they both provide a difference field with peak of -16 dBi.

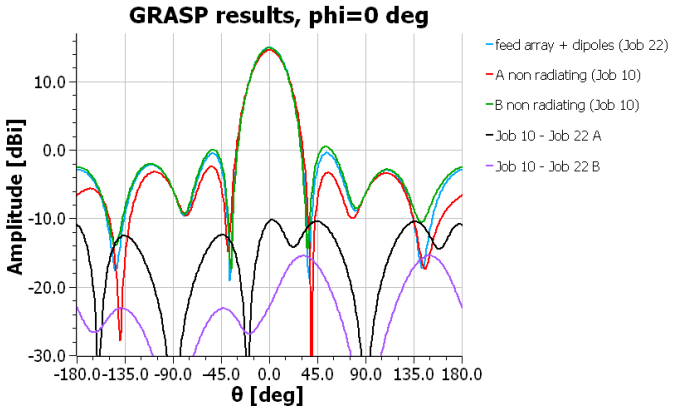

Figure 8. Amplitude of the field obtained by GRASP with MoM: Job 10 and Job 22.

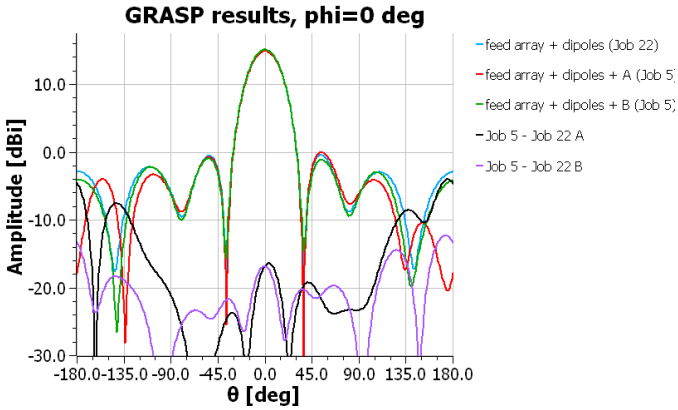

Figure 9. Amplitude of the field obtained by GRASP with MoM: Job 5 and Job 22.

IV. 3D RECONSTRUCTION WITH GRASP INPUT FIELD

The field of Figure 7 is used as input to DIATOOL and the equivalent currents are reconstructed on a box enclosing the feed array and the support frame, for configuration A and B.

A. Configuration A

In Figure 10 a plot of the amplitude of the reconstructed total electric currents is shown. The four patches are clearly identified on the top face of the box. Lower currents are also visible on the lateral faces. The field radiated by these currents was then computed and compared with the input field shown in Figure 7. It was found, as expected, that these two fields coincided, and that their complex difference was below -30 dBi.

Later on, the full box was replaced by two boxes, on top of each other and sharing one face, see Figure 11 to the left, and the current reconstruction was repeated with the same input field. The reconstructed currents were the same of Figure 10 and the field radiated by these currents coincided again with the input pattern of Figure 7.

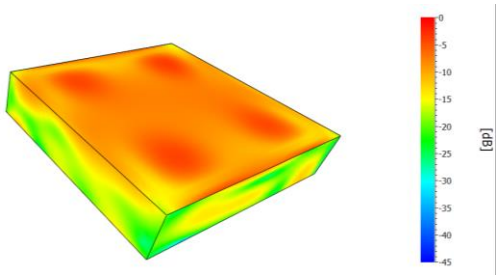

Figure 10. Amplitude of the total electric currents reconstructed on a box circumscribing the antenna and the support frame of configuration A.

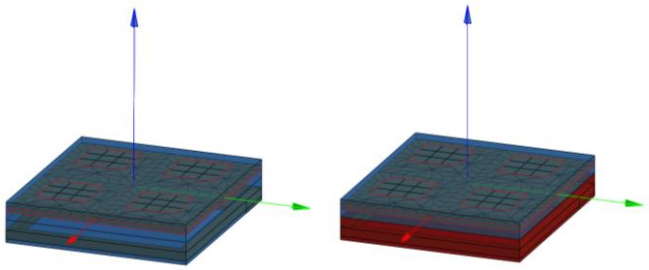

Figure 11. Reconstruction surface given by two boxes sharing one face: the reconstructed currents on both boxes radiate to the far-field (to the left), only the currents on the upper box radiate to the far-field (to the right).

Finally, the currents on the lower box, where the frame is located, were imposed as “non radiating”, as depicted in Figure 11 to the right, and the field given by the currents on the upper box alone was computed and compared with the field radiated by the full box of Figure 10. The result can be seen in Figure 12 for the phi=0 cut.

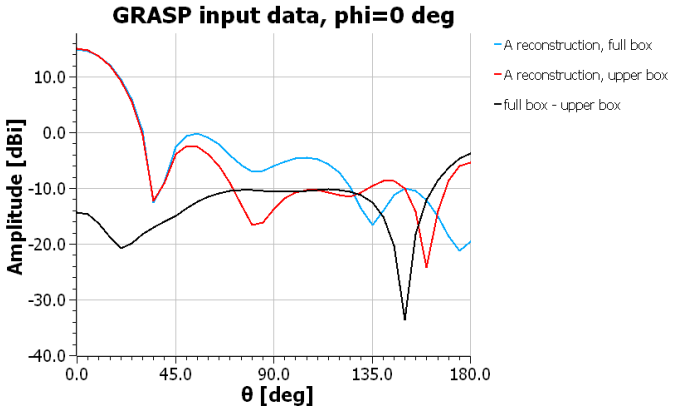

Figure 12. Field given by the reconstructed currents of DIATOOL: configuration A and GRASP input.

It is seen that the amplitude of the field given by the full box currents and the upper box currents coincides in the main lobe and differs for theta larger than 45 deg. The complex difference in the main beam has a maximum value equal to -

14 dBi. If we then compare the field from the upper box reconstruction with the field computed by GRASP when the frame A does not radiate (Job 10) and with the field given by the patch and dipoles, without frame and without coupling (Job 22), we obtain Figure 13. This indicates that the field computed by DIATOOL with lower box non-radiating is definitely closer in the main beam to the ideal reference of Job 22 than Job 10.

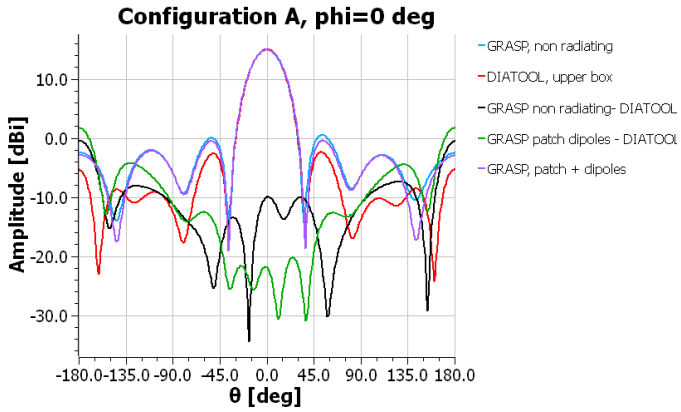

Figure 13. Field given by the reconstructed currents of DIATOOL when only the upper box radiates compared to GRASP fields.

B. Configuration B

We repeated the same procedure for configuration B, using the same upper box of configuration A and obtained Figure 14.

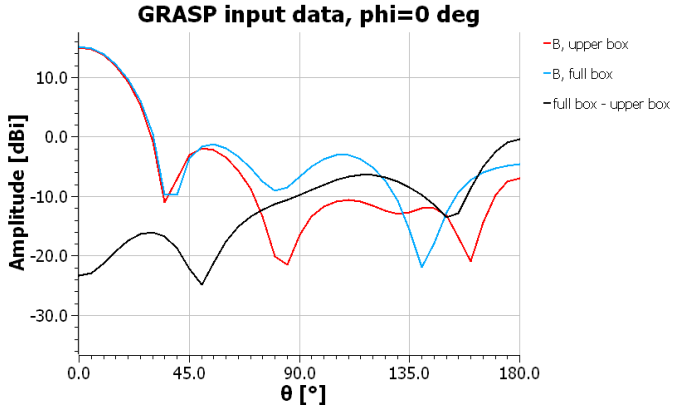

Figure 14. Field given by the reconstructed currents of DIATOOL: configuration B and GRASP input.

The complex difference has a maximum value equal to -16 dBi and a mean value of -20 dBi in the main beam. If we compare the field from the upper box reconstruction with the field computed by GRASP when the frame B was non-radiating (Job 10) and with the field given by the patch and dipoles, without frame and without coupling (Job 22), we obtain Figure 15. Like for configuration A, the field computed by DIATOOL with lower box non-radiating is closer in the main beam to the ideal reference of Job 22 than Job 10, though the green curve has now a maximum of -15 dBi instead of the -20 dBi of Figure 13. Finally, the pattern given by the upper box of configuration A and the upper box of configuration B are compared, obtaining Figure 16. It is seen that the difference curve has a maximum of -20 dBi in the main lobe, which is clearly better than the -11 dBi of Figure 7. We can conclude that the filtering of the currents on the lower box generates for both configurations two fields that in the main beam are very close to the ideal reference field of Job 22 (green line of Figure 13 and Figure 15). At the same time these two fields are closer to each other compared to what they were in Figure 7.

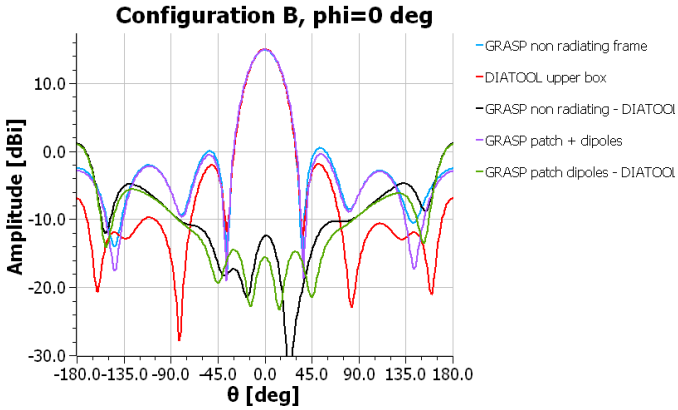

Figure 15. Field given by the reconstructed currents of DIATOOL when only the upper box radiates compared to GRASP fields.

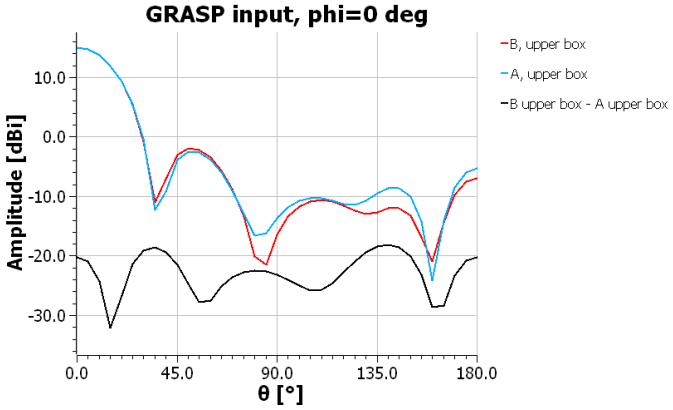

Figure 16. Field given by the reconstructed currents of DIATOOL, when only the upper box radiates, for configuration A and B.

V. 3D RECONSTRUCTION WITH MEASURED INPUT FIELD

The same procedure was applied to configuration A and B considering now as input to DIATOOL the field measured at the DTU-ESA facility. Figure 17 shows the field radiated by the reconstructed currents of DIATOOL for configuration A and Figure 18 for configuration B. The field radiated by the upper box of configuration A and B, when the lower box is non-radiating is shown in Figure 20. Figure 20 almost coincides with Figure 16, obtained with simulated input fields.

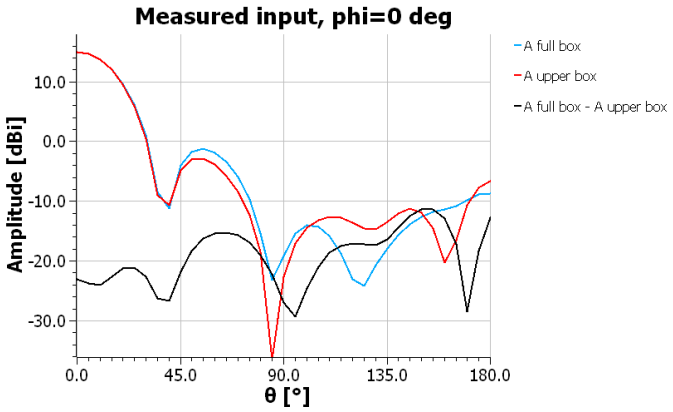

Figure 17. Field given by the reconstructed currents of DIATOOL: configuration A and measured input.

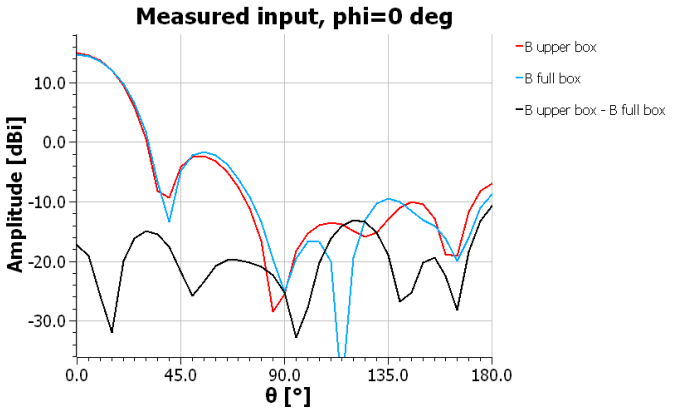

Figure 18. Figure 19. Field given by the reconstructed currents of DIATOOL: configuration B and measured input.

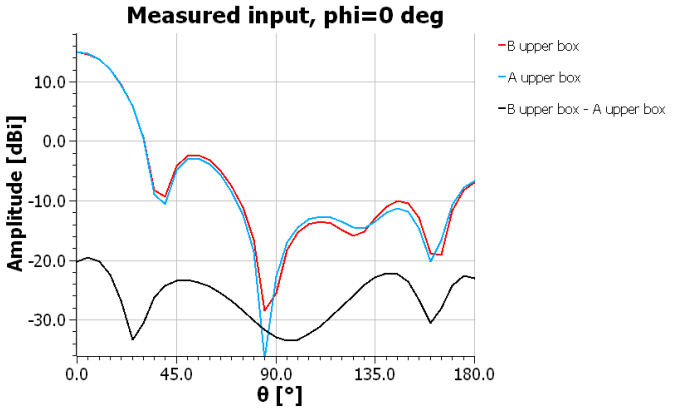

Figure 20. Field given by the reconstructed currents of DIATOOL, when only the upper box radiates, for configuration A and B.

The difference curve has a peak of -20 dBi in the main lobe, corresponding to a peak-to-peak variation of the measured pattern of ±0.15 dB at the pattern peak level. This value is clearly better than the ±0.3 dB of the input measured field of Figure 4. On the basis of the results of Section 4, we conclude that the pattern of Figure 20 provided by DIATOOL has filtered the effect of the supporting frame from the measured field.

VI. CONCLUSIONS

Spherical near-field measurements of the feed prototype of the BIOMASS showed a too large effect of the metallic support frame used to mount the feed array on the antenna tower. The support frame gave rise to a peak-to-peak variation of the measured pattern of ±0.3 dB at the pattern peak level: a too large value in itself, and also relative to the other uncertainty contributions of the applied measurement technique.

A GRASP model of the feed prototype was thus made in order to evaluate the effect of the support frame. It was seen that the differences observed in the measured field could only be reproduced if an unwanted radiation of the array feeding network was considered.

The feed array measured data, and the simulated data generated by the GRASP software replicating the series of measurements, where then read into DIATOOL. The 3D reconstruction was used to evaluate, and later filter, the contribution of the support frame on two boxes on top of each other, sharing one face and conformal to the antenna. The support frame was contained in the lower box. The post-processing performed by DIATOOL by imposing the currents on the lower box as non-radiating provided a cleaned pattern where the peak-to-peak variation at the pattern peak level was reduced to ±0.15 dB, both for measured and GRASP data. Moreover, the cleaned pattern turned out to be very close to the ideal reference field generated by GRASP when no supporting frame was present.

We can thus conclude that DIATOOL can be used to remove the effect of the test support frame from the measured pattern. This cleaned pattern can then be used to illuminate the large deployable reflector, and thus provide the required overall performances of the P-band synthetic aperture radar.

REFERENCES

[1] E. Jørgensen, P. Meincke, O. Borries, and M. Sabbadini, "Processing of measured fields using advanced inverse method of moments algorithm", Proc. of the 33rd ESA Antenna Workshop, ESTEC, Noordwijk, The Netherlands, 2011.

[2] E. Jørgensen, P. Meincke, C. Cappellin, and M. Sabbadini, "Improved source reconstruction technique for antenna diagnostics", Proc. of the 32nd ESA Antenna Workshop, ESTEC, Noordwijk, The Netherlands, 2010.

[3] European Space Agency: The Living Planet Programme – Earth Explorers. Available from http://www.esa.int/Our_Activities/Observing_the_Earth/The_Living_Planet_Programme

[4] R. Mizzoni, G. Orlando and P. Valle, "Unfurlable Reflector SAR Antenna at P-Band", Proc. of EuCAP 2009, Berlin, Germany.

[5] S. Pivnenko, et al, "Measurement campaigns for selection of optimum on-ground performance verification approach for large deployable reflector antenna", Proc. of 34th AMTA Symp., Bellevue, WA, USA, 2012.

[6] S. Pivnenko, O.S. Kim, and O. Breinbjerg: Study of very large aperture P-band antenna performance verification methodology and facilities. SR9: Summary Report. Technical University of Denmark, Dept. of Electrical Engineering, May 2012. (R 758, 37p).